

Learning Vehicle Trajectory Uncertainty

Barak Or, *Member, IEEE*, and Itzik Klein, *Senior Member, IEEE*

Abstract—The linear Kalman filter is commonly used for vehicle tracking. This filter requires knowledge of the vehicle trajectory and the statistics of the system and measurement models. In real-life scenarios, prior assumptions made while determining those models do not hold. As a consequence, the overall filter performance degrades and in some situations the estimated states diverge. To overcome the uncertainty in the vehicle kinematic trajectory modeling, additional artificial process noise may be added to the model or different types of adaptive filters may be employed. This paper proposes a hybrid adaptive Kalman filter based on model and machine learning algorithms. First, recurrent neural networks are employed to learn the vehicle’s geometrical and kinematic features. In turn, those features are plugged into a supervised learning model, thereby providing the actual process noise covariance to be used in the Kalman framework. The proposed approach is evaluated and compared to six other adaptive filters using the Oxford RobotCar dataset. The proposed framework can be implemented in other estimation problems to accurately determine the process noise covariance in real-time scenarios.

Index Terms—Adaptive estimation, autonomous vehicles, machine learning, Kalman filter, vehicle tracking, trajectory modeling, adaptive estimation, recurrent neural networks, long short-term memory.

I. INTRODUCTION

The Kalman filter (KF) is widely used for vehicle tracking tasks [1]–[8] and vehicle trajectory smoothing [4], [9]–[12]. One of the challenges to consider when applying a KF for tracking applications is the modeling of the vehicle trajectory, as expressed by the system matrix and associated process noise covariance. Commonly, the constant velocity (CV) or a constant acceleration (CA) models are employed for a wide range of vehicle tracking problems [1], [12]–[15]. In the CV model, the underlying assumption is that the vehicle travels with constant velocity. The addition of process noise turns the model to a nearly CV model allowing the filter to cope with varying velocity. In the same manner, CA assumes constant vehicle acceleration and the addition of process noise turns the model to a nearly CA model allowing the filter to cope with varying acceleration. That is, the added process noise covariance enables the filter to cope with unmodeled vehicle dynamics (for example, as additional states) or perturbations up to some magnitude level [16]. Nevertheless, such a choice of trajectory modeling ensures a Gauss-Markov (GM) process and provides an optimal estimation [17], [18]. As long as the underlying model assumptions hold, the filter accuracy is satisfactory. However, in practice, the vehicle dynamics can differ from the model assumptions leading to a mismatch between the modeling and the actual behavior of the

vehicle. As a consequence, the tracking filter performance degrades, and, in some situations, diverges. In automated vehicle perspective, it might result in a loss of information on the vehicle location that could potentially lead to an accident [19]. Therefore, model uncertainty, namely process noise covariance determination, is considered critical in the pre-processing phase of the KF [17], [20]. Generally, setting

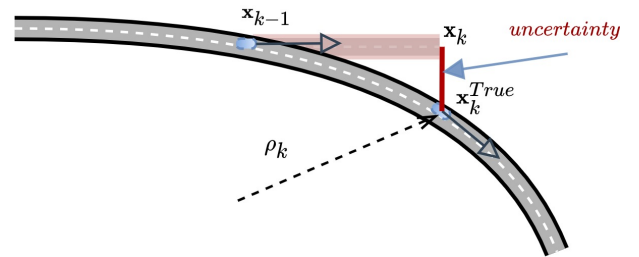


Fig. 1. Trajectory modeling error demonstration. The vehicle position at timestamp k is predicted to maintain a straight line, according to the trajectory model (CV). However, its true position at time k is along the road, where it performed a circular motion (along a circle with radius ρ) to stay on the road. This tracking error is a direct result of the designer uncertainty for the trajectory model (red vertical line), which must be considered with appropriate Gaussian noise.

higher values in the process noise covariance results in short memory behavior of the filter. In such situations, the kinematic model assumptions are less important since a high-magnitude random noise drives the trajectory model and the filter favors the external measurements when calculating the filter gain. In some situations, such a process leads to a non-optimal trajectory estimation. On the other hand, choosing lower values for the process noise covariance leads to a long memory filter behavior. In that scenario, the kinematic model is of high importance and there is (almost) no gap for modeling errors. Thus, a sudden change in the vehicle state, even for a fraction of time, might result in low estimation performance and filter divergence.

Instead of choosing constant values for the process noise covariance matrix, adaptive process noise covariance approaches may be employed [17], [21]–[24]. The three most common approaches are: 1) the innovation-based method, where the innovation quantity is used together with the Kalman gain to calibrate the matrix [25], 2) modified scaling, where the measurement noise covariance matrix is known and used to keep the trajectory uncertainty noise matrix scaled [26], and 3) generative learning, where the system transition matrix model is used to calculate and correct model error every two successive steps [16]. Although many works addressed this issue, the problem of optimal trajectory modeling by tuning the trajectory uncertainty process noise covariance is still considered unsolved [17].

Submitted: July 2021. Revised: March 2022.

Barak Or and Itzik Klein are with the Department of Marine Technologies, Charney School of Marine Science, University of Haifa, Haifa, 3498838, Israel (e-mail: barakorr@gmail.com, kitzik@univ@haifa.ac.il).

Machine learning (ML) and deep learning (DL) approaches [27] show state-of-the-art performances in various fields such as computer vision [28], natural language processing [29], and pedestrian dead reckoning [30].

Recent works, addressing model uncertainty, explore the possibility of using ML/DL approaches. Learning approaches suggest including a loss function that contains the process noise covariance, both directly and indirectly [16]. Here, the learning approach learns the covariance matrix parameters online. Yet, the resulting time to converge is too long, as the entire history of the tracking process is considered. In [9], a curve-fitting approach was proposed for tuning trajectory uncertainty noise matrix using a neural network. However, the method demands a training set with ground truth for the entire trajectory, which makes it unrealistic for real-time tracking when considering a new environment, for example. In this paper, a hybrid adaptive linear Kalman filter, based on machine learning algorithms and the model-based Kalman filter equations is proposed to cope with the model uncertainty in the vehicle tracking problem. Although an end-to-end network is simpler to implement, it does not give any intuition to the problem and acts as a black box. On the other hand, hybrid approaches rely on well-established model based theory while adding the benefits of data-driven approaches by replacing a single operation in the model based solution. The proposed hybrid approach consists of two steps. First, recurrent neural networks are employed to learn the vehicle's geometrical and kinematic features namely, the road curvature and vehicle speed. Secondly, these features are inserted into a supervised learning (SL) model providing the actual process noise covariance to use in the Kalman framework. The proposed approach can be applied in online scenarios. To demonstrate its performance, vehicle tracking using CV and CA models are considered. The proposed approach is analyzed and compared to six other adaptive filters using the Oxford RobotCar database [31]. Results show the benefits of implementing the proposed hybrid learning model approach.

The main contribution of this paper is a learning-based scheme which utilizes the road curvature, vehicle speed, and noise measurement covariance as features to accurately estimate the model uncertainty and thereby improving the vehicle tracking performance.

The rest of this paper is organized as follows: Section II deals with the problem formulation for CV and CA models and the tracking filter and its trajectory uncertainty as well as the common approaches to adapt the trajectory uncertainty noise matrix. Section III presents the trajectory uncertainty learning scheme, where the feature engineering, dataset generation process, and online tuning scheme with the KF are discussed. Section IV presents the results, and Section V gives the conclusions.

II. PROBLEM FORMULATION

A. Tracking Filter

The linear discrete KF is presented.

Initial conditions are

$$\begin{aligned}\hat{\mathbf{x}}_0 &= \mathcal{E}[\mathbf{x}_0] \\ \mathbf{P}_0 &= \mathcal{E}\left[(\mathbf{x}_0 - \mathcal{E}[\mathbf{x}_0])(\mathbf{x}_0 - \mathcal{E}[\mathbf{x}_0])^T\right]\end{aligned}\quad (1)$$

where \mathbf{x}_0 is the initial state vector, $\hat{\mathbf{x}}_0$ is the initial estimate state vector, and \mathbf{P}_0 is the initial covariance error. The state estimate propagation is given by

$$\hat{\mathbf{x}}_k^- = \Phi \hat{\mathbf{x}}_{k-1} \quad (2)$$

where $\hat{\mathbf{x}}_k^-$ is the estimate of the current state k , $\hat{\mathbf{x}}_{k-1}$ is the estimate of the previous state $k-1$, and Φ is the discrete system matrix. The error covariance propagation is given by

$$\mathbf{P}_k^- = \Phi \mathbf{P}_{k-1} \Phi^T + \mathbf{Q}_k \quad (3)$$

where \mathbf{P}_{k-1} is the estimate from the previous state, $k-1$, \mathbf{P}_k^- is the estimate from the current state, k , and \mathbf{Q} is the trajectory uncertainty noise matrix (covariance). When a measurement is available, an update is made, according to the following equations set (4) – (7). The Kalman gain is given by

$$\mathbf{K}_k = \mathbf{P}_k^- \mathbf{H}^T (\mathbf{H} \mathbf{P}_k^- \mathbf{H}^T + \mathbf{R}_k)^{-1}. \quad (4)$$

The innovation vector is defined by

$$\nu_k = \mathbf{z}_k - \mathbf{H} \hat{\mathbf{x}}_k^- \quad (5)$$

The state estimate update is given by

$$\hat{\mathbf{x}}_k = \hat{\mathbf{x}}_k^- + \mathbf{K}_k \nu_k \quad (6)$$

and the error covariance update (correction) is

$$\mathbf{P}_k = (\mathbf{I} - \mathbf{K}_k \mathbf{H}) \mathbf{P}_k^- \quad (7)$$

The choice of \mathbf{Q} can be divided into three categories:

- 1) $\mathbf{Q} = \mathbf{0}$: might lead to a non-stabilized/optimal filter

Theorem 1. *If $\mathbf{Q}_k \rightarrow \mathbf{0}$, then the Kalman gain is a function of the weighted trajectory model, the error covariance, \mathbf{P}_{k-1} , and the measurement noise covariance only. In that manner, (4) is rewritten as*

$$\mathbf{K}_k = \left[(\Phi \mathbf{P}_{k-1} \Phi^T)^{-1} + \mathbf{H}^T \mathbf{R}_k^{-1} \mathbf{H} \right]^{-1} \mathbf{H}^T \mathbf{R}_k^{-1} \quad (8)$$

- 2) $\|\mathbf{Q}\|_2 \rightarrow \infty$ (flat prior): leads to not considering the model, so the KF uses the measurement only.

Theorem 2. *If $\|\mathbf{Q}\|_2 \rightarrow \infty$, then the Kalman gain reduces to*

$$\mathbf{K}_k = [\mathbf{H}^T \mathbf{R}_k^{-1} \mathbf{H}]^{-1} \mathbf{H}^T \mathbf{R}_k^{-1} \quad (9)$$

and the state estimate (6) reduces to the weighted least squares estimator (LSE):

$$\hat{\mathbf{x}}_k = [\mathbf{H}^T \mathbf{R}_k^{-1} \mathbf{H}]^{-1} \mathbf{H}^T \mathbf{R}_k^{-1} \mathbf{z}_k. \quad (10)$$

A demonstration is presented in Figures 2 and 3, where a vehicle trajectory was set to follow a circle trajectory model and the KF trajectory model was set to a CV model (a straight line). Here, the Kalman gain did not consider

the mismatch between Φ and the actual motion made caused by the vehicle (Figure 2). Also, the KF prediction suffered from a large error (Figure 3).

- 3) An arbitrary positive matrix can be set manually or using one of the methods presented in Section II.C.

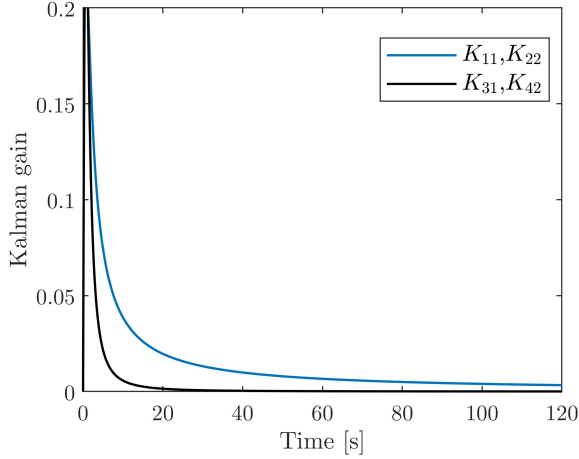


Fig. 2. The Kalman gain with $\mathbf{Q} = \mathbf{0}$ converges accurately despite the wrong trajectory modeling with a CV model, while in practice the movement was circular.

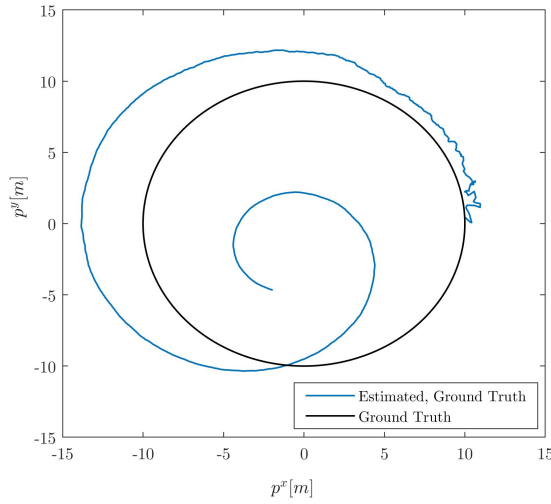


Fig. 3. The resulting trajectory when setting $\mathbf{Q} = \mathbf{0}$ in the Kalman filter with a wrong trajectory model with a CV model, while in practice the movement was circular.

B. CV and CA Models

Any trajectory model includes some level of uncertainty. The simplest modeling approach is to set a linear trajectory motion with an additional uncertainty term. This assumption has important properties such as the Markov-Gauss process, where the current state depends only on the last state, allowing optimal implementation of the KF for accurate tracking. For example, consider an autonomous vehicle tracking problem using a CV model as demonstrated in Figure 1. In practice,

the vehicle moves along a circle. The velocity vector points towards the tangential direction due to the circular motion. However, according to the assumed trajectory, the vehicle should be moving in a straight direction.

Commonly, two trajectory models are considered for vehicle motion: firstly, a CV model, which assumes that a vehicle moves mostly in the same velocity; and secondly, a CA model, which assumes a vehicle moves mostly in the same acceleration. The CV can be described by a smaller state-space than the CA, so it might be less sensitive to modeling errors. Alongside, the CA model considers the velocity changes with an additional state for the acceleration. The CV and CA models are provided by

$$p_{k+1}^i = p_k^i + v_k^i \Delta t + \sqrt{q_k^i} n_k^i \quad (11)$$

and

$$p_{k+1}^i = p_k^i + v_k^i \Delta t + \frac{1}{2} a_k^i \Delta t^2 + \sqrt{q_k^i} n_k^i \quad (12)$$

where p is the vehicle's position, v is the vehicle's velocity, a is the vehicle's acceleration, Δt is the step size (assumed to be constant), q is the uncertainty term, n is a standard Gaussian white noise, k is the time step, and $i \in \{x, y\}$ is the axis index. The state space of the CV model is given by

$$\mathbf{x} = [\mathbf{p}^T \quad \mathbf{v}^T]^T \in \mathbb{R}^{4 \times 1} \quad (13)$$

with the corresponding transition matrix

$$\Phi^{CV} = \begin{bmatrix} \mathbf{I}_{2 \times 2} & \Delta t \mathbf{I}_{2 \times 2} \\ \mathbf{0} & \mathbf{I}_{2 \times 2} \end{bmatrix} \in \mathbb{R}^{4 \times 4} \quad (14)$$

where $\mathbf{I}_{n \times n}$ is the identity matrix, and the trajectory noise covariance matrix is

$$\mathbf{Q}_k^{CV} = \left[\begin{array}{c|c} \mathbf{0}_{2 \times 2} & \mathbf{0}_{2 \times 2} \\ \hline \mathbf{0}_{2 \times 2} & \begin{matrix} q_k^x & 0 \\ 0 & q_k^y \end{matrix} \end{array} \right] \in \mathbb{R}^{4 \times 4}. \quad (15)$$

The state space of the CA model is given by

$$\mathbf{x} = [\mathbf{p}^T \quad \mathbf{v}^T \quad \mathbf{a}^T]^T \in \mathbb{R}^{6 \times 1} \quad (16)$$

with the corresponding transition matrix

$$\Phi^{CA} = \begin{bmatrix} \mathbf{I}_{2 \times 2} & \Delta t \mathbf{I}_{2 \times 2} & \frac{1}{2} \Delta t^2 \mathbf{I}_{2 \times 2} \\ \mathbf{0}_{2 \times 2} & \mathbf{I}_{2 \times 2} & \Delta t \mathbf{I}_{2 \times 2} \\ \mathbf{0}_{2 \times 2} & \mathbf{0}_{2 \times 2} & \mathbf{I}_{2 \times 2} \end{bmatrix} \in \mathbb{R}^{6 \times 6} \quad (17)$$

and the trajectory noise covariance matrix is

$$\mathbf{Q}_k^{CA} = \left[\begin{array}{cc|c} \mathbf{0}_{2 \times 2} & \mathbf{0}_{2 \times 2} & \mathbf{0}_{2 \times 2} \\ \mathbf{0}_{2 \times 2} & \mathbf{0}_{2 \times 2} & \mathbf{0}_{2 \times 2} \\ \hline \mathbf{0}_{2 \times 2} & \mathbf{0}_{2 \times 2} & \begin{matrix} q_k^x & 0 \\ 0 & q_k^y \end{matrix} \end{array} \right] \in \mathbb{R}^{6 \times 6} \quad (18)$$

Formulating it as a vector results in

$$\mathbf{x}_{k+1} = \Phi \mathbf{x}_k + \sqrt{\mathbf{Q}_k} \mathbf{n}_k \quad (19)$$

where \mathbf{x}_k is the state vector at time step k , and Φ is the dynamic transition matrix. We design \mathbf{Q}^{CV} , \mathbf{Q}^{CA} matrices with only non-zero terms in the highest order of the state, and using (2) will result in additive noise for all states.

The error between the true state, \mathbf{x}_k^{True} , and the model state, \mathbf{x}_k , is defined as

$$\tilde{\mathbf{x}}_k \triangleq \mathbf{x}_k - \mathbf{x}_k^{True}. \quad (20)$$

The discrete measurement model is given by

$$z_k^i = p_k^i + \sqrt{r_k^i} w_k^i, \quad i \in \{x, y\} \quad (21)$$

where r_k^i is the measurement noise covariance and w_k^i is a white Gaussian discretized noise. The observation matrix for the CV model is given by

$$\mathbf{H}^{CV} = \begin{bmatrix} \mathbf{I}_{2 \times 2} & \mathbf{0}_{2 \times 2} \end{bmatrix} \in \mathbb{R}^{2 \times 4}. \quad (22)$$

The observation matrix for the CA model is given by

$$\mathbf{H}^{CA} = \begin{bmatrix} \mathbf{I}_{2 \times 2} & \mathbf{0}_{2 \times 2} & \mathbf{0}_{2 \times 2} \end{bmatrix} \in \mathbb{R}^{2 \times 6}. \quad (23)$$

The corresponding measurement noise covariance matrix for both models is given by

$$\mathbf{R}_k^{CV} = \mathbf{R}_k^{CA} = \begin{bmatrix} r_k^x & 0 \\ 0 & r_k^y \end{bmatrix} \in \mathbb{R}^{2 \times 2}. \quad (24)$$

The measurement equation in the state space is given by

$$\mathbf{z}_k = \mathbf{H}\mathbf{x}_k + \sqrt{\mathbf{R}_k} \mathbf{w}_k \quad (25)$$

where no correlations between measurement and trajectory noises is assumed ($\mathbb{E}[\mathbf{n}_k \mathbf{w}_k^T] = \mathbf{0}$). The goal is to estimate the vehicle trajectory based on noisy position measurements. For simplicity, a perfect knowledge of the measurement model only is assumed.

C. Common Adaptive Approaches

The common approaches for adaptive tuning of \mathbf{Q} are innovation based methods, generative learning, and modified scaling:

- 1) **Innovation-based methods.** The most common approach to estimate \mathbf{Q} in an adaptive KF framework was suggested in [25]; it is based on the innovation vector (5). The innovation matrix for a window size ξ is defined by

$$\mathbf{C}_k \triangleq \frac{1}{\xi} \sum_{j=k-\xi+1}^k \nu_j \nu_j^T. \quad (26)$$

The choice of ξ is critical: if a small window size is selected, the averaging might be insufficient. From the other side, if ξ is too large, there is a delay in the innovation calculation due to the time elapsed from past trajectory points. The innovation matrix is used together with the Kalman gain, \mathbf{K} , to adapt \mathbf{Q} :

$$\hat{\mathbf{Q}}_k = \mathbf{K}_k \mathbf{C}_k \mathbf{K}_k^T. \quad (27)$$

- 2) **Generative learning.** A naive approach for learning the filter parameters (and specifically \mathbf{Q}) [16] requires access to the full state vector, and is generally considered inapplicable (due to difficulty in measuring all state variables).

Generative learning demands the maximization of the likelihood function of all the data, using

$$\mathbf{Q}^* = \arg \max_{\mathbf{Q}} \left\{ \begin{array}{l} -M \log [2\pi \mathbf{Q}] \\ - \sum_{k=1}^M (\mathbf{x}_k - \Phi \mathbf{x}_{k-1})^T \mathbf{Q}^{-1} (\mathbf{x}_k - \Phi \mathbf{x}_{k-1}) \end{array} \right\}, \quad (28)$$

so minimization of a quadratic function with \mathbf{Q}^{-1} as a factor is achieved. The optimal solution of (28) is given by

$$\mathbf{Q}_k^* = \frac{1}{M} \sum_{k=1}^M (\mathbf{x}_k - \Phi \mathbf{x}_{k-1}) (\mathbf{x}_k - \Phi \mathbf{x}_{k-1})^T. \quad (29)$$

- 3) **Scaling method.** A scaling method of the covariance matrices was proposed in [32] and [33]. The Kalman gain, \mathbf{K} , depends on the ratio of \mathbf{Q} and \mathbf{R} . Hence, if one of them is known, the other can be estimated. For example, if \mathbf{R} is known, \mathbf{Q} can be estimated by satisfying the following condition for covariance matching:

$$\mathbf{H} \mathbf{P}_k^- \mathbf{H}^T + \mathbf{R}_k = \mathbf{C}_k. \quad (30)$$

The core idea behind the scaling method is that if the estimated covariance of ν_k in (26) is much larger than the theoretical covariance, then \mathbf{Q} should be increased and vice versa. This deviation from the optimal value is considered using a scaling factor α_k , defined as

$$\alpha_k = \frac{\text{trace} \left(\left[\frac{1}{\xi} \sum_{j=k-\xi+1}^k \nu_j \nu_j^T \right] - \mathbf{R}_k \right)}{\text{trace} (\mathbf{H} \mathbf{P}_k^- \mathbf{H}^T)} \quad (31)$$

leading to a scaled covariance of

$$\hat{\mathbf{Q}}_k = \sqrt{\alpha_k} \hat{\mathbf{Q}}_{k-1}. \quad (32)$$

III. LEARNING TRAJECTORY UNCERTAINTY

A. Motivation

Modeling the vehicle's trajectory as a CV or CA model allows the filter designer to modify the trajectory process noise matrix with respect to the curvature, vehicle speed, and measurement noise covariance. In this approach, the trajectory is divided into a finite set of curves, $\mathbf{L}_k \in \mathcal{L}$. For each curve, the averaged curvature, averaged velocity, and measurement noise can be calculated. The curve can be represented by the vehicle estimated states:

$$\mathbf{L}_k = \{\hat{p}_i^x, \hat{p}_i^y\}_{i=k-N}^{k-1} \in \mathbb{R}^{2 \times N} \quad (33)$$

where \mathbf{L}_k is a vehicle states segment, represented by N points. Using the curvature operator, (34), the curve, as a function of the vehicle states, is mapped into a segment curvature, $\bar{\kappa}_k$:

$$\bar{\kappa}_k(\mathbf{L}_k) = \frac{1}{N} \left[\sum_{j=k}^{k+N-1} \kappa_j \right] \quad (34)$$

where κ_j is defined by

$$\kappa_j \triangleq \frac{\det(\mathbf{L}'_j, \mathbf{L}''_j)}{\|\mathbf{L}_j\|^3}, \quad (35)$$

L'_k and L''_k are the first and second order derivatives, respectively.

From a tracking point of view, such formulation of a curve, L_k , can be interpreted as a road section k provided by N points with curvature κ_k , as demonstrated in Figure 4. Obviously, if

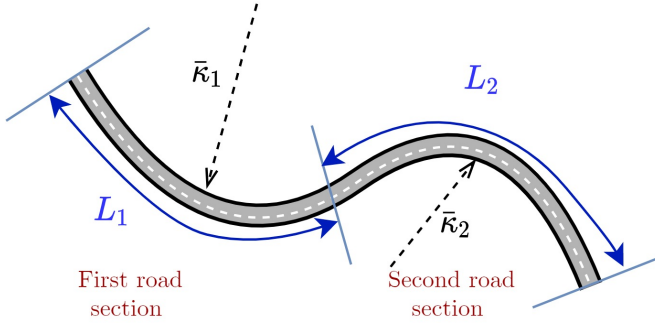


Fig. 4. A general trajectory consisting of two sections with different geometrical properties showing the length and curvature of each. The road curvature is defined in (35).

$\kappa \rightarrow \infty$, the trajectory is a straight line and no compensation for the geometrical mismatch between the trajectory model and the actual vehicle trajectory should be applied. However, where the mismatch is significant (i.e., $\kappa > 0.01[1/m]$), compensation for the inaccuracy of the assumed model should be applied, hence \mathbf{Q} should be tuned accordingly.

B. Proposed Approach

A novel approach is derived for online learning the trajectory model uncertainty in terms of the process noise covariance matrix, with geometric and kinematic features. It is argued that an online calculation of such features together with a pre-trained model allows a better determination of the trajectory uncertainty model, and hence the process noise covariance matrix. In the proposed approach, the last N vehicle position states are inserted into a bi-directional long short-term memory (LSTM) network to regress the trajectory segment curvature. Then, the speed is calculated using the averaged estimated velocity components in the last N states, and inserted, together with the measurement noise covariance, into an additional learning model (fine tree, GPR, or Support Vector Machine) to determine \mathbf{Q}_k^* . Finally, the KF uses the optimal \mathbf{Q}_k^* and outputs its current estimated state, $\hat{\mathbf{x}}_k$, as shown in Figure 5.

Estimating the curvature, $\hat{\kappa}$, in real-time vehicle tracking scenarios is not a trivial task, as the measured vehicle position and their estimates are noisy. Hence, an LSTM network is used to estimate the averaged curvature along a curve [34]; specifically, a bi-directional LSTM, as described below. The curvature alone is not sufficient for tuning \mathbf{Q}_k ; therefore, two additional features are considered: 1) the measurement noise covariance and 2) the vehicle speed. These three features are combined into an ML model to determine the optimal \mathbf{Q}_k according to the last N measurements and their estimate.

C. Learning Framework

The proposed learning framework has two steps: 1) The Bi-LSTM model used for online curvature learning 2) A feature-

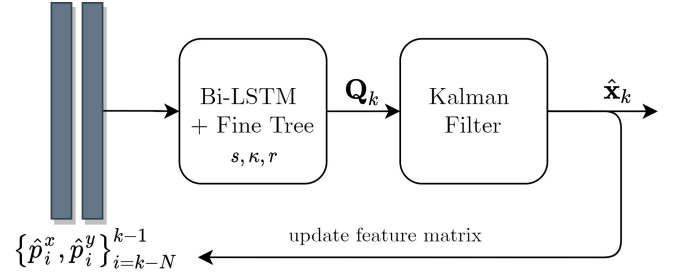


Fig. 5. Proposed approach block diagram: N last estimated position states are inserted into a bi-directional LSTM. Then, the vehicle speed is calculated and inserted together with the measurement noise covariance into a fine tree model to determine \mathbf{Q}_k^* . Finally, the KF uses the optimal \mathbf{Q}_k^* and outputs its current state estimate, $\hat{\mathbf{x}}_k$.

based supervised learning model to estimate the process noise covariance. Here, the curvature from step 1) is used as one of the features. The proposed learning framework is illustrated in Figure 8.

1) Bi-LSTM based model for online curvature learning:

We employed a DL-based model to generalize the geometric curvature property. The main advantage of using DL is the generalization capability of intrinsic properties appearing in sequential data. The LSTM is a modification of a recurrent neural network (RNN) where feedback connections are added. Every LSTM unit with input (α_t) contains a cell (C_t), an input gate (i_t), an output gate (o_t), and a forget gate (f_t). The cell's output (h_t) is usually flattened and inserted into fully connected layers. The cell remembers values over intervals and the three gates regulate the flow of information in and out of the cell, as shown in Figure 6. Generally, when using

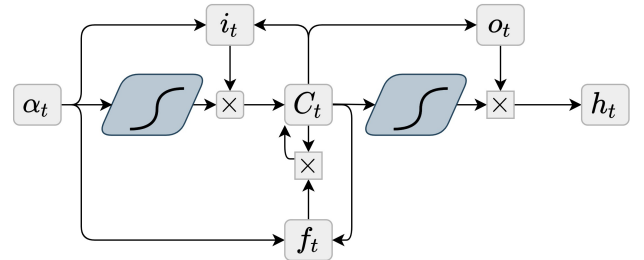


Fig. 6. Classical LSTM unit with input, forget, and output gates.

an LSTM network, the information passes only backward, where only casual time-dependent properties are calculated (only past information). One method to circumvent it is to pass the information forward through an additional layer, thereby allowing the network to capture additional information. This approach is known as the bi-directional LSTM (Bi-LSTM) [34] and is illustrated in Figure 7. Here, two time blocks are presented for two successive time steps, each having two LSTM blocks with 100 units. One passes information forward and the other passes information backward. Their output is combined using a Sigmoid activation function to obtain their final output (m), inserted into a fully connected layer with 30 hidden units, and eventually combined with the additional

features.

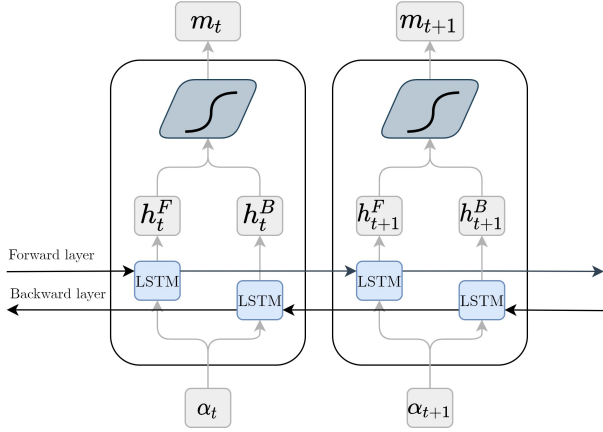


Fig. 7. Illustration of two time steps in a bi-directional LSTM model. The output of the forward layer (h_t^F) is combined with the output of the backward layer (h_t^B) using a Sigmoid activation function.

An example on how to produce an adaptive learning curvature module is provided in Figure 8. A circle with a predefined radius, equals to 10[m], is simulated (black line). The measurement noise magnitude was set to 1[m²] both in x and y directions, and the vehicle speed was set to 10[m/s]. Applying the KF (2)-(7) created the estimated trajectory (blue). Each 20 samples along the circle were stored with their respective optimal κ^* , as the ground truth label. By repeating this procedure to create the dataset, allowed eventually, the bi-LSTM model establishment.

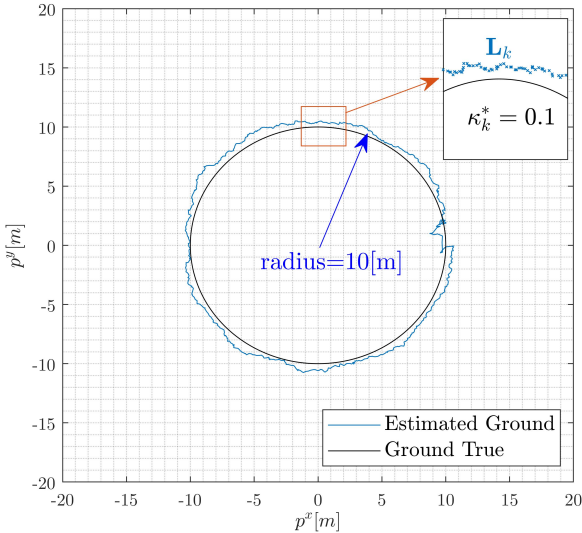


Fig. 8. An example of a trajectory included in the dataset.

2) *Learning models configuration*: Three types of features are used as input to the SL model:

1) Road curvature (as described in the previous subsection):

$$\hat{\kappa}_k = f_{Bi-LSTM} \left(\{ \mathbf{x}_j \}_{j=k-N}^{k-1} \right) \quad (36)$$

where κ_k is the road curvature at time k .

2) Vehicle speed:

$$\hat{s}_k = \sqrt{(\hat{v}_k^x)^2 + (\hat{v}_k^y)^2} \quad (37)$$

where \hat{s}_k is the estimated vehicle speed velocity at time k .

3) Measurement noise covariance:

$$\mathbf{R}_k = \begin{bmatrix} r & 0 \\ 0 & r \end{bmatrix} \quad (38)$$

where r is a constant noise variance.

The SL model's output is q^* :

$$q_k^* = f_{SL}(\hat{\kappa}_k, r, \hat{s}) \quad (39)$$

3) *Learning algorithm summary*: Algorithm (1) summarizes the online tuning process of \mathbf{Q}_k using both the Bi-LSTM and SL model steps. In step 5, \mathbf{Q}_k is calculated using the vehicle speed, the measurement noise covariance, and the curvature estimation. An hedging mechanism enforces \mathbf{Q}_k as a positive diagonal matrix. Finally, the KF is updated and states are stored. Step 5 expresses the proposed learning framework including the Bi-LSTM network and the SL model. Figure 9 shows the flow of steps 2-5 including the network structure. In the results section we compare between several types of learning models using Algorithm 1.

Algorithm 1 SL-based model for online tuning of \mathbf{Q}_k

Input: $\mathbf{x}_0, \mathbf{P}_0, \mathbf{Q}_0, \mathbf{R}, \Phi, \mathbf{H}, \mathbf{z}, \xi$

Output: $\hat{\mathbf{x}}_k$

1: Initialization: $\hat{\mathbf{x}}_0 = \mathbf{0}, \hat{\mathbf{Q}}_1 = \mathbf{Q}_0$

LOOP Process

2: **for** $k = 1$ to M **do**

3: Propagate

$$\hat{\mathbf{x}}_k^-, \mathbf{P}_k^- = f(\Phi, \hat{\mathbf{x}}_{k-1}, \mathbf{P}_{k-1}^-, \hat{\mathbf{Q}}_k)$$

4: Calculate gain

$$\mathbf{K}_k = f(\mathbf{P}_k^-, \mathbf{H}, \mathbf{R})$$

5: Estimating speed

$$\hat{s}_k = \sqrt{(\hat{v}_k^x)^2 + (\hat{v}_k^y)^2}$$

6: **if** $k > \xi$ **then**

7: Update $\hat{\mathbf{Q}}_k$

$$\hat{\mathbf{Q}}_k = f_{SL}(s, r, \{ \mathbf{x}_j \}_{j=k-\xi+1}^k)$$

8: Hedging \mathbf{Q}

$$\hat{\mathbf{Q}}_k \leftarrow \hat{\mathbf{Q}}_k \odot \mathbf{I}$$

$$[Q_{ij}]_k \leftarrow [Q_{ij}]_k \mathcal{I}_{\{ [Q_{ij}]_k > 0 \}}$$

9: **else**

10: $\mathbf{Q}_k = \mathbf{Q}_0$

11: **end if**

12: Update

$$\hat{\mathbf{x}}_k, \mathbf{P}_k^+ = f(\hat{\mathbf{x}}_k^-, \mathbf{K}_k, \mathbf{z}_k, \mathbf{H}, \hat{\mathbf{x}}_{k-1}, \mathbf{P}_{k-1}^-, \hat{\mathbf{Q}}_k)$$

13: Return $\hat{\mathbf{x}}_k$

14: **end for**

D. Datasets

To establish the relationship between vehicle speed, measurement noise, road curvature, and their optimal \mathbf{Q}^* matrix, the following assumptions were made:

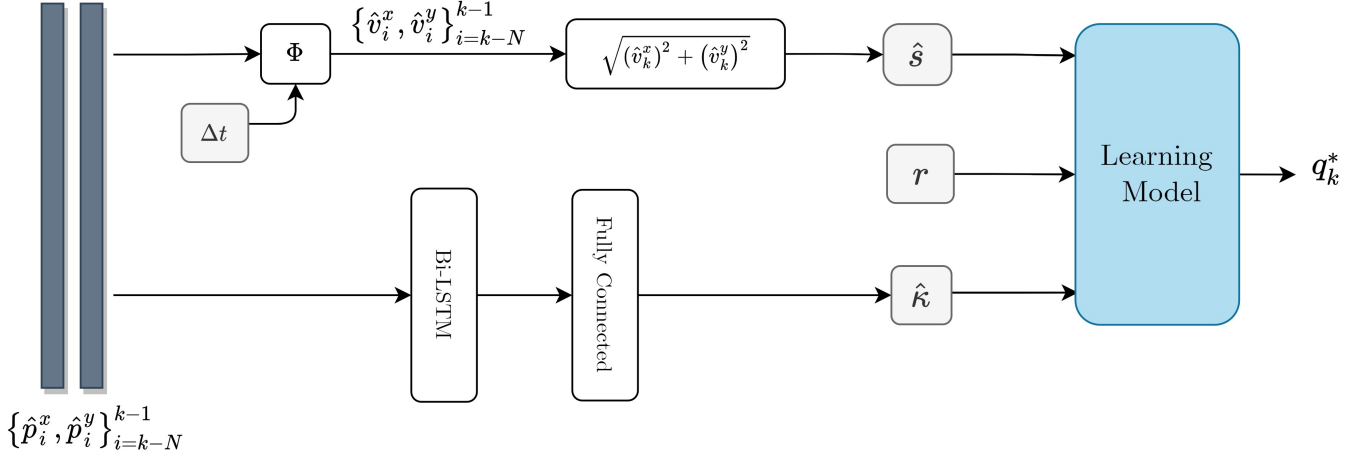


Fig. 9. The proposed learning model with its two stages includes three features: speed (s), noise magnitude (r), and curvature (κ), which are estimated through a Bi-LSTM based model. The speed estimate depends on the problem modeling where Φ represents the discrete form of the chosen system matrix and Δt is the step size. The logistic regression model's input are position estimate vectors in both x and y directions of size N , and the final output is a sub-optimal trajectory uncertainty noise term \hat{q}_k^* .

- 1) Fixed altitude: All vehicle's trajectories are two dimensional.
- 2) All vehicle's trajectories can be represented as a superposition of curves, each with corresponding curvatures κ_k .
- 3) Vehicle speed values vary between $2[m/s]$ and $40[m/s]$.
- 4) Measurement noise variance is identical in both directions, where $r_x = r_y = r$, and noise is assumed to be zero mean white Gaussian noise.
- 5) The KF step size is constant.

Following these assumptions, we constructed simulated circle trajectories with different radiuses ($1/\kappa$), measurement noise, and speed, as provided in Table I.

The circles were obtained using the following circular trajectory model:

$$p_k^x = (1/\kappa) \cos(\omega t_k) \quad (40)$$

$$p_k^y = (1/\kappa) \sin(\omega t_k) \quad (41)$$

where t_k is the time propagated by

$$t_k = t_{k-1} + \Delta t \quad (42)$$

and the angular velocity, ω , is defined by the road's curvature, κ , and the vehicle's speed, s , as

$$\omega = s\kappa. \quad (43)$$

Equations (40) – (43) combined with the KF equations (1) – (7) were simulated; once for the CV model (14) – (15), (22), (24) and once for the CA model (17) – (18), (23) – (24).

Using the parameters in Table 1, a grid search for the optimal q^* value was performed. For example, the set $\{\kappa, r, s\}_j$ was run 34 times for different q candidates (the list is provided in the appendix). For each candidate, q_j , MC with 50 iterations was simulated to obtain an accurate calculation of the mean square error (MSE) measure.

Finally, the value that minimizes the MSE was stored with its set values as the ground truth values.

$$\mathbf{Q}^* = \arg \min_{\mathbf{Q}} \tilde{x}^T \mathbf{Q} \tilde{x} \quad (44)$$

where

$$\mathbf{Q} = \begin{bmatrix} \mathbf{0}_{(m-d) \times (m-d)} & \mathbf{0}_{(m-d) \times d} \\ \mathbf{0}_{d \times (m-d)} & q \mathbf{I}_{d \times d} \end{bmatrix} \in \mathbb{R}^{m \times m} \quad (45)$$

m is the state vector dimension, and d is the physical dimension, thus in our 2D scenarios, $d = 2$. For example, one case of finding the optimal q^* value for $\kappa = 0.05[1/m]$, $s = 10[m/s]$, $r = 1[m^2]$ in a CV trajectory model is presented in Figure 10. The optimal value received a position root mean square error (46) of less than $0.4[m]$ with $q^* = 0.04$.

In the first step of the proposed learning framework, Section

TABLE I
PARAMETERS USED FOR CREATING THE DATASET.

| Parameter | Values Range | Value step |
|--------------------------|---|---|
| Speed | $2 < s < 40 \left[\frac{m}{s} \right]$ | $\Delta s = 2 \left[\frac{m}{s} \right]$ |
| Curvature | $1/200 < \kappa < 1 \left[\frac{1}{m} \right]$ | $\Delta \kappa = 1/10 \left[\frac{1}{m} \right]$ |
| Measurement noise covar. | $0.2 < r < 4 \left[m^2 \right]$ | $\Delta r = 0.2 \left[m^2 \right]$ |

III.C, the goal is to reconstruct the curvature given a short curve ($N = 20$). To that end, another massive dataset of 240,000 examples was created. Each example contains twenty points (features), simulated along a defined circle with a known radius and its curvature (label). These examples were defined according to Table I. This dataset was divided in a ratio of 80/20 for the train/test procedures (192,000/48,000), where for every epoch, 24,000 shuffled examples were fed in with their respective curvature parameters. The training used the Adam optimizer with a gradient threshold, for 30 epochs (8 iterations each). In this setup, the trained model achieved a curvature root mean square error of $0.02 \left[\frac{1}{m} \right]$ on the test set.

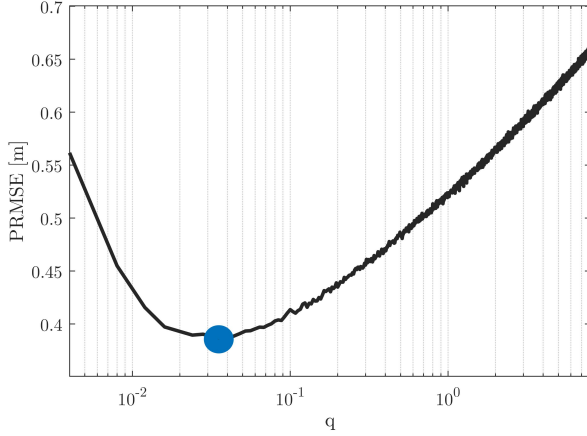


Fig. 10. An example of finding the optimal q^* in a sense of minimum PRMSE.

IV. RESULTS

Two error metrics were used to evaluate model performance:

- Position root mean square error is

$$PRMSE = \sqrt{\frac{1}{T_k} \sum_{i \in \{x,y\}} \left[\sum_{k=1}^{T_k} \left(p_k^{i, True} - \hat{p}_k^i \right)^2 \right]} \quad (46)$$

where T_k is the total time steps.

- Position mean absolute error:

$$PMAE = \frac{1}{T_k} \sum_{i \in \{x,y\}} \left[\sum_{k=1}^{T_k} \left| \left(p_k^i \right)^{True} - \hat{p}_k^i \right| \right] \quad (47)$$

A. Classical Adaptive Models

The classical adaptive models, presented in Section II.C, were evaluated using Monte Carlo (MC) simulations with 100 iterations on the RobotCar [31], for various measurement noise levels, as summarized in Table II. The RobotCar trajectories, with the 31 minutes/10[km] vehicle driving scenarios employed in this paper, are illustrated in Figure 11.

First, we ran the cases where $q \rightarrow 0$ (Theorem 1), which were translated for practical reasons into $q = 10^{-9}$ to avoid numerical issues. This case represents the high confidence level of the KF designer, where large position error was obtained for all noise levels for both CV and CA models, as expected. Secondly, we ran the cases where $q \rightarrow \infty$ (Theorem 2), which were translated into $q = 10^9$ to avoid numerical issues. This case represents a flat prior, where the trajectory model is not considered, and obtained a position error much closer to the defined measurement noise covariance. The chosen constant values were the same as the measurement noise covariances: $q = r$.

The innovation-based \mathbf{Q} tuning approach, generative learning (with four/six terms along the diagonal of \mathbf{Q}), and scaling method were run with a fixed window size of $\xi = 10$. No major change for different window sizes was detected. All adaptive approaches yield better performance than taking

$q \rightarrow 0$, $q \rightarrow \infty$, and constant values. The lower PRMSE and PMAE was obtained for the scaling method with the CV model.

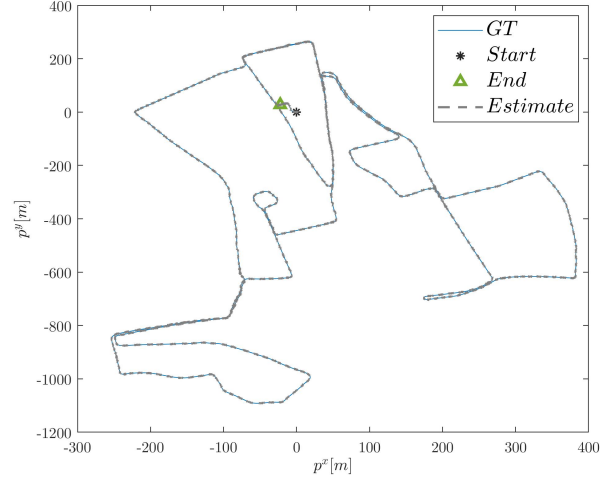


Fig. 11. Several trajectories from the Oxford RobotCar dataset were employed in this work. They include 31 minutes and 10 kilometers of vehicle driving scenarios. The estimated trajectory was obtained using the CA fine tree Bi-LSTM based $Q(r, s, \kappa)$ Regression model, where $r = 0.5[m^2]$.

B. Learning-based Models

1) *Training models:* Applying learning-based models can be made after training them. Several regression and classification models were trained and analyzed for both for CV and CA datasets (IV.B-D) to determine which one to employ in the proposed approach. The motivation to include also the classification models, aside the regression models, is their higher robustness as there exist a finite set of accessible values for q . The training/test procedure included the five-fold cross-validation approach [35] for obtaining robust trained models. The regression models included decision trees, linear regression, Gaussian process regression (GPR) [36], and support vector machine regression [37]. Classification models were also trained, including decision trees, k nearest neighborhood (KNN), SVM, and Naive Bayes. The training and testing was made on the dataset as defined in Section III.D. It was observed that an optimized GPR, with a non-isotropic Matern 5/2 kernel, obtained the lowest RMSE of $0.67[m]$ and thus was selected as a possible candidate from all regression models for the CV dataset. Also, SVM with a cubic kernel was selected for the classification approach, with an accuracy of 72%. The confusion matrix is presented in Figure 12, where it is shown that most of the values were predicted correctly. For the CA dataset, a fine tree was selected as a possible candidate as it obtained the lowest RMSE of $0.83[m]$ out of all regression models. Also, SVM with a quadratic kernel was selected for the classification approach, as it obtained an accuracy of 74.5%. The confusion matrix is given in Figure 13, where it is shown that most of the values were predicted correctly.

2) *Integrating the ML models with the KF:* Eventually, these ML models should be integrated with the KF in a real-time manner to predict and tune the sub-optimal \mathbf{Q}_k matrix.

TABLE II
COMPARISON OF CLASSICAL MODELS FOR A TRAJECTORY OF OXFORD ROBOTCAR WITH VARYING MEASUREMENT NOISE COVARIANCE.

| Model / Error metric | PRMSE [m] | PMAE [m] | PRMSE [m] | PMAE [m] | PRMSE [m] | PMAE [m] |
|--|----------------|----------------|--------------|--------------|--------------|--------------|
| Measurement noise cov. | $r = 0.5[m^2]$ | $r = 0.5[m^2]$ | $r = 2[m^2]$ | $r = 2[m^2]$ | $r = 4[m^2]$ | $r = 4[m^2]$ |
| CV $\mathbf{Q} \rightarrow 0$ | 98.4 | 103 | 125 | 132 | 143 | 151 |
| CA $\mathbf{Q} \rightarrow 0$ | 23.6 | 24.5 | 32.0 | 33.0 | 37.5 | 38.4 |
| CV $\ \mathbf{Q}\ _2 \rightarrow \infty$ (LSE) | 0.99 | 1.12 | 1.99 | 2.25 | 2.82 | 3.19 |
| CA $\ \mathbf{Q}\ _2 \rightarrow \infty$ (LSE) | 1.00 | 1.12 | 2.00 | 2.25 | 2.82 | 3.18 |
| CV constant \mathbf{Q} | 0.64 | 0.73 | 1.12 | 1.26 | 1.47 | 1.66 |
| CA constant \mathbf{Q} | 0.62 | 0.70 | 1.13 | 1.27 | 1.53 | 1.72 |
| CV innovation-based \mathbf{Q} | 0.64 | 0.70 | 1.09 | 1.20 | 1.42 | 1.56 |
| CA innovation-based \mathbf{Q} | 0.55 | 0.61 | 0.97 | 1.08 | 1.30 | 1.45 |
| CV generative learning | 0.82 | 0.95 | 1.64 | 1.97 | 2.30 | 2.80 |
| CA generative learning | 0.82 | 0.96 | 1.64 | 1.98 | 2.31 | 2.83 |
| CV scaling method | 0.57 | 0.60 | 1.01 | 1.09 | 1.35 | 1.46 |
| CA scaling method | 0.61 | 0.65 | 1.09 | 1.18 | 1.45 | 1.57 |

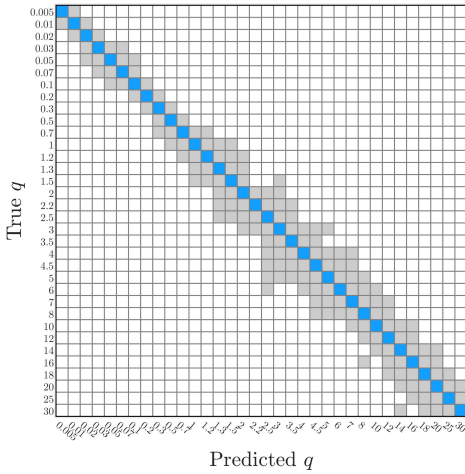


Fig. 12. Confusion matrix for SVM classifier with a cubic kernel, where the problem is formulated as a classification task (CV dataset).

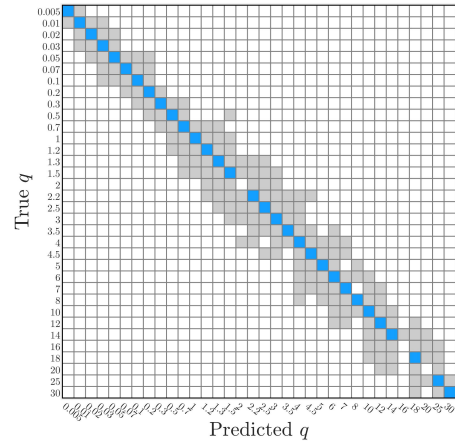


Fig. 13. Confusion matrix for the SVM classifier with a quadratic kernel, where the problem is formulated as a classification task (CA dataset).

The GPR, SVM, and fine tree models for both CV and CA models were evaluated for two cases:

- Using only two features: the measurement noise covariance (r) and speed (s). In that manner, the Bi-LSTM network is not required in the process.
- Same as the first case with the addition of the curvature (κ) feature. In this case, the Bi-LSTM based model was plugged into the scheme, as shown in Figure 9.

Similarly to the classical models, we used the RobotCar dataset to evaluate the ML-based model. Results are summarized in Table III.

The minimum PRMSE and PMAE for $r = 0.5[m^2]$ was obtained for the CA model with the fine tree + Bi-LSTM regression approach. Here, a PRMSE of $0.49[m]$ was measured, which was a reduction of 11% from the CV GPR model (PRMSE= $0.54[m]$). Hence, for a low covariance measurement noise of $r = 0.5[m^2]$, adding the curvature as a feature for determining \mathbf{Q}_k improves the filter's performance.

Increasing the measurement noise covariance, $r = 2[m^2]$, results in a lower PRMSE= $0.85[m]$ and PMAE= 0.95 for a CA model with the SVM approach (only (s, r)) as features. The

reason for not considering the curvature lies in the difficulty of reconstructing the averaged curvature from a noisy series. However, the obtained PRMSE is lower by 16% than the one obtained using the scaling method with the CV model (PRMSE= $1.01[m]$).

Lastly, increasing the measurement noise covariance to $r = 4[m^2]$ results in a lower PRMSE= $1.11[m]$ and PMAE= $1.25[m]$ for a CV model with the GPR approach. This PRMSE is lower by 20% than the one achieved using the CA innovation-based \mathbf{Q} approach. We considered the case of perfect curvature, κ_{GT} , to evaluate the curvature-based models performance. The results are also summarized in Table III, where there is a minor improvement of no more than 2% PRMSE reduction while the κ_{GT} is considered. Hence, the Bi-LSTM based curvature learning was well trained and provides an accurate curvature in a real time setting.

C. Discussion

The classical adaptive models results are provided in Section VI.A and our hybrid learning-based models results in Section VI.B. The performance of the adaptive model-based approaches is superior to model based approaches with con-

TABLE III
LEARNING-BASED MODELS COMPARISON FOR A TRAJECTORY OF OXFORD ROBOTCAR WITH VARYING MEASUREMENT NOISE COVARIANCE.

| Model / Error metric | PRMSE [m] | PMAE [m] | PRMSE [m] | PMAE [m] | PRMSE [m] | PMAE [m] |
|---|----------------|----------------|--------------|--------------|--------------|--------------|
| Measurement noise covariance | $r = 0.5[m^2]$ | $r = 0.5[m^2]$ | $r = 2[m^2]$ | $r = 2[m^2]$ | $r = 4[m^2]$ | $r = 4[m^2]$ |
| CV GPR-based $\mathbf{Q}(r, s)$ Reg. | 0.54 | 0.57 | 0.86 | 0.97 | 1.11 | 1.25 |
| CV SVM-based $\mathbf{Q}(r, s)$ Class. | 0.63 | 0.71 | 0.94 | 1.05 | 1.16 | 1.30 |
| CA fine tree-based $\mathbf{Q}(r, s)$ Reg. | 0.62 | 0.70 | 1.13 | 1.27 | 1.52 | 1.72 |
| CA SVM-based $\mathbf{Q}(r, s)$ Class. | 0.63 | 0.70 | 0.85 | 0.95 | 1.15 | 1.29 |
| CV GPR BiLSTM-based $\mathbf{Q}(r, s, \hat{\kappa})$ Reg. | 0.58 | 0.65 | 1.02 | 1.14 | 1.37 | 1.52 |
| CV SVM BiLSTM-based $\mathbf{Q}(r, s, \hat{\kappa})$ Class. | 0.55 | 0.60 | 1.01 | 1.08 | 1.34 | 1.43 |
| CA fine tree BiLSTM-based $\mathbf{Q}(r, s, \hat{\kappa})$ Reg. | 0.49 | 0.55 | 0.97 | 1.08 | 1.30 | 1.46 |
| CA SVM BiLSTM-based $\mathbf{Q}(r, s, \hat{\kappa})$ Class. | 0.56 | 0.62 | 0.98 | 1.09 | 1.38 | 1.53 |
| CV GPR BiLSTM-based $\mathbf{Q}(r, s, \kappa_{GT})$ Reg. | 0.58 | 0.64 | 1.02 | 1.14 | 1.37 | 1.52 |
| CV SVM BiLSTM-based $\mathbf{Q}(r, s, \kappa_{GT})$ Class. | 0.55 | 0.61 | 0.99 | 1.08 | 1.30 | 1.43 |
| CA fine tree BiLSTM-based $\mathbf{Q}(r, s, \kappa_{GT})$ Reg. | 0.52 | 0.59 | 0.97 | 1.09 | 1.31 | 1.46 |
| CA SVM BiLSTM-based $\mathbf{Q}(r, s, \kappa_{GT})$ Class. | 0.55 | 0.62 | 1.02 | 1.14 | 1.39 | 1.54 |

stant process noise values, as they try to capture the vehicle current dynamics and the measurement noise statistic in a real-time. The innovation-based model and the scaling method are better than the generative learning, as they achieved lower PRMSE and PMAE for all tested measurement noise covariance values. For $r = 0.5[m^2]$, the CA innovation-based \mathbf{Q} obtained PRMSE of $0.55[m]$ and PMAE of $0.61[m]$. Thus an improvements of 11% and 13% was obtained in the PRMSE and PMAE, respectively, compared to model based approaches with constant process noise values.

The learning-based models were pre-trained to capture the non-linearity and other uncertainty properties, once using the relationship between the measurement noise covariance and vehicle speed and once with the addition of the road curvature as a feature. The hybrid learning-based models achieved better performance than the adaptive models as they consider additional learnt information during the training phase. Without the curvature feature, CV GPR-based $\mathbf{Q}(r, s)$ Reg. model, obtained a PRMSE of $0.54[m]$ and PMAE of $0.57[m]$, for $r = 0.5[m^2]$. This model improves the PRMSE with 13% and the PMAE with 19% compared to model based approaches with constant process noise values. Including the road curvature feature, the best performance for the CA model was archived with the fine tree BiLSTM-based $\mathbf{Q}(r, s, \hat{\kappa})$. It obtained a PRMSE of $0.49[m]$ and PMAE of $0.55[m]$, for $r = 0.5[m^2]$. Hence, it improves the PRMSE with 21% and the PMAE with 21.5% compared to model based approaches from the CA constant process noise values and improves the PRMSE with 11% and the PMAE with 10% from the adaptive model based methods.

V. CONCLUSIONS

The proper choice of the trajectory process noise covariance matrix is critical for achieving high accuracy when implementing the discrete linear filter in vehicle tracking scenarios. The commonly used solution is to choose constant matrix parameters or to use any classical adaptive approach. A practical hybrid ML-based framework to tune a sub-optimal matrix online, was proposed in this research. The framework combines kinematic and geometrical features, where a BiLSTM-based model is used to estimate the curvature in real

time and a supervised learning model was used to merge it with the measurement noise covariance and vehicle speed. In the proposed framework, the model needs to be trained only once, regardless of the nature of the vehicle motion or road trajectory. This fact makes it suitable to use in other scenarios. Extensive simulations on the RobotCar dataset were made to demonstrate the efficiency of the suggested scheme. We obtained state-of-the-art results for each noise value compared to classical adaptive KF approaches; a position RMSE lower than $0.5[m]$ was obtained using a Kalman filter with a constant acceleration trajectory model by plugging in SVM + BiLSTM, given only three features: vehicle speed, measurement noise covariance, and road curvature.

The proposed approach can be implemented in real-time vehicle tracking problems. Those can include autonomous vehicles, robotics platforms, or drones.

APPENDIX

A. List of q candidates

$$\mathcal{Q} = \left\{ \begin{array}{l} 0.005, 0.01, 0.02, 0.03, 0.05, 0.07, 0.1, 0.2, \\ 0.3, 0.5, 0.7, 1, 1.2, 1.3, 1.5, 2, 2.5, 3, 3.5, 4, \\ 4.5, 5, 6, 7, 8, 10, 12, 14, 16, 18, 20, 25, 30 \end{array} \right\} \quad (48)$$

REFERENCES

- [1] Y. Bar-Shalom, X. R. Li, and T. Kirubarajan, *Estimation with applications to tracking and navigation: theory algorithms and software*. John Wiley & Sons, 2004.
- [2] R. E. Kalman, "A new approach to linear filtering and prediction problems," *Journal of Basic Engineering*, vol. 82, no. 1, pp. 35–45, 1960.
- [3] D. N. Aloi and O. V. Korniyenko, "Comparative performance analysis of a Kalman filter and a modified double exponential filter for GPS-only position estimation of automotive platforms in an urban-canyon environment," *IEEE Transactions on Vehicular Technology*, vol. 56, no. 5, pp. 2880–2892, 2007.
- [4] L. Xiong, X. Xia, Y. Lu, W. Liu, L. Gao, S. Song, and Z. Yu, "IMU-based automated vehicle body sideslip angle and attitude estimation aided by GNSS using parallel adaptive Kalman filters," *IEEE Transactions on Vehicular Technology*, vol. 69, no. 10, pp. 10668–10680, 2020.
- [5] D. Pavkovic, J. Deur, and I. Kolmanovsky, "Adaptive kalman filter-based load torque compensator for improved si engine idle speed control," *IEEE Transactions on Control Systems Technology*, vol. 17, no. 1, pp. 98–110, 2008.

- [6] Z. Qin, L. Chen, J. Fan, B. Xu, M. Hu, and X. Chen, "An improved real-time slip model identification method for autonomous tracked vehicles using forward trajectory prediction compensation," *IEEE Transactions on Instrumentation and Measurement*, vol. 70, pp. 1–12, 2021.
- [7] A. Motroni, A. Buffi, P. Nepa, and B. Tellini, "Sensor-fusion and tracking method for indoor vehicles with low-density uhf-rfid tags," *IEEE Transactions on Instrumentation and Measurement*, vol. 70, pp. 1–14, 2020.
- [8] R. Xiong, L. Li, C. Zhang, K. Ma, X. Yi, and H. Zeng, "Path tracking of a four-wheel independently driven skid steer robotic vehicle through a cascaded ntsm-pid control method," *IEEE Transactions on Instrumentation and Measurement*, vol. 71, pp. 1–11, 2022.
- [9] S. Baek, C. Liu, P. Watta, and Y. L. Murphey, "Accurate vehicle position estimation using a Kalman filter and neural network-based approach," in *2017 IEEE Symposium Series on Computational Intelligence (SSCI)*. IEEE, 2017, pp. 1–8.
- [10] H. Marzbani, H. Khayyam, C. N. To, a. V. Quoc, and R. N. Jazar, "Autonomous vehicles: Autodriver algorithm and vehicle dynamics," *IEEE Transactions on Vehicular Technology*, vol. 68, no. 4, pp. 3201–3211, 2019.
- [11] B. Cui, X. Wei, X. Chen, J. Li, and L. Li, "On sigma-point update of cubature kalman filter for gnss/fins under gnss-challenged environment," *IEEE Transactions on Vehicular Technology*, vol. 68, no. 9, pp. 8671–8682, 2019.
- [12] B. Or, B.-Z. Bobrovsky, and I. Klein, "Kalman filtering with adaptive step size using a covariance-based criterion," *IEEE Transactions on Instrumentation and Measurement*, vol. 70, pp. 1–10, 2021.
- [13] M. M. Olama, S. M. Djouadi, I. G. Papageorgiou, and C. D. Charalambous, "Position and velocity tracking in mobile networks using particle and kalman filtering with comparison," *IEEE Transactions on Vehicular Technology*, vol. 57, no. 2, pp. 1001–1010, 2008.
- [14] Y. Fu, C. Li, F. R. Yu, T. H. Luan, and Y. Zhang, "A decision-making strategy for vehicle autonomous braking in emergency via deep reinforcement learning," *IEEE transactions on vehicular technology*, vol. 69, no. 6, pp. 5876–5888, 2020.
- [15] S. C. Stubberud, K. A. Kramer, and J. A. Geremia, "Online sensor modeling using a neural kalman filter," *IEEE Transactions on Instrumentation and Measurement*, vol. 56, no. 4, pp. 1451–1458, 2007.
- [16] P. Abbeel, A. Coates, M. Montemerlo, A. Y. Ng, and S. Thrun, "Discriminative Training of Kalman Filters," in *Robotics: Science and systems*, vol. 2, 2005, p. 1.
- [17] L. Zhang, D. Sidoti, A. Bienkowski, K. R. Pattipati, Y. Bar-Shalom, and D. L. Kleinman, "On the identification of noise covariances and adaptive Kalman filtering: A new look at a 50 year-old problem," *IEEE Access*, vol. 8, pp. 59362–59388, 2020.
- [18] A. H. Jazwinski, *Stochastic processes and filtering theory*. Courier Corporation, 2007.
- [19] J. Nilsson, M. Brännström, E. Coelingh, and J. Fredriksson, "Lane change maneuvers for automated vehicles," *IEEE Transactions on Intelligent Transportation Systems*, vol. 18, no. 5, pp. 1087–1096, 2016.
- [20] A. Artunedo, J. Villagra, J. Godoy, and M. D. del Castillo, "Motion planning approach considering localization uncertainty," *IEEE Transactions on Vehicular Technology*, vol. 69, no. 6, pp. 5983–5994, 2020.
- [21] F. Aghili and C.-Y. Su, "Robust relative navigation by integration of ICP and adaptive Kalman filter using laser scanner and IMU," *IEEE/ASME Transactions on Mechatronics*, vol. 21, no. 4, pp. 2015–2026, 2016.
- [22] A. Mohamed and K. Schwarz, "Adaptive Kalman filtering for INS/GPS," *Journal of geodesy*, vol. 73, no. 4, pp. 193–203, 1999.
- [23] Y. Yang and W. Gao, "An optimal adaptive Kalman filter," *Journal of Geodesy*, vol. 80, no. 4, pp. 177–183, 2006.
- [24] G. Galben, "New three-dimensional velocity motion model and composite odometry–inertial motion model for local autonomous navigation," *IEEE Transactions on Vehicular Technology*, vol. 60, no. 3, pp. 771–781, 2011.
- [25] R. Mehra, "On the identification of variances and adaptive Kalman filtering," *IEEE Transactions on Automatic Control*, vol. 15, no. 2, pp. 175–184, 1970.
- [26] M. Saha, R. Ghosh, and B. Goswami, "Robustness and sensitivity metrics for tuning the extended Kalman filter," *IEEE Transactions on Instrumentation and Measurement*, vol. 63, no. 4, pp. 964–971, 2013.
- [27] I. Goodfellow, Y. Bengio, and A. Courville, *Deep learning*. MIT Press, 2016.
- [28] Y. Guo, Y. Liu, A. Oerlemans, S. Lao, S. Wu, and M. S. Lew, "Deep learning for visual understanding: A review," *Neurocomputing*, vol. 187, pp. 27–48, 2016.
- [29] E. Cambria and B. White, "Jumping NLP curves: A review of natural language processing research," *IEEE Computational Intelligence Magazine*, vol. 9, no. 2, pp. 48–57, 2014.
- [30] O. Asraf, F. Shama, and I. Klein, "Pdrnet: A deep-learning pedestrian dead reckoning framework," *IEEE Sensors Journal*, 2021.
- [31] W. Maddern, G. Pascoe, C. Linegar, and P. Newman, "1 year, 1000 km: The Oxford RobotCar dataset," *The International Journal of Robotics Research*, vol. 36, no. 1, pp. 3–15, 2017.
- [32] W. Ding, J. Wang, C. Rizos, and D. Kinlyside, "Improving adaptive Kalman estimation in GPS/INS integration," *The Journal of Navigation*, vol. 60, no. 3, p. 517, 2007.
- [33] C. Hu, W. Chen, Y. Chen, D. Liu *et al.*, "Adaptive Kalman filtering for vehicle navigation," *Journal of Global Positioning Systems*, vol. 2, no. 1, pp. 42–47, 2003.
- [34] F. A. Gers, J. Schmidhuber, and F. Cummins, "Learning to forget: Continual prediction with LSTM," *Neural Computation*, vol. 12, no. 10, pp. 2451–2471, 2000.
- [35] P. Refaeilzadeh, L. Tang, and H. Liu, "Cross-validation," *Encyclopedia of Database Systems*, vol. 5, pp. 532–538, 2009.
- [36] M. Seeger, "Gaussian processes for machine learning," *International Journal of Neural Systems*, vol. 14, no. 02, pp. 69–106, 2004.
- [37] O. Chapelle and V. Vapnik, "Model selection for support vector machines," *Advances in Neural Information Processing Systems*, vol. 12, pp. 230–236, 1999.

Barak Or (Member, IEEE) received B.Sc. (2016) and M.Sc. (2018) degrees in aerospace engineering and a B.A. in economics and management (2016, cum laude) from the Technion–Israel Institute of Technology. Barak is studying for his Ph.D. at the University of Haifa. His research interests include inertial navigation, deep learning, sensor fusion, and estimation theory.



Itzik Klein (Senior Member, IEEE) received the B.Sc. and M.Sc. degrees in Aerospace Engineering from the Technion - Israel Institute of Technology, Haifa, Israel, in 2004 and 2007, respectively, and a Ph.D. degree in Geo-information Engineering from the Technion - Israel Institute of Technology, in 2011. He is currently an Assistant Professor, heading the Autonomous Navigation and Sensor Fusion Lab, at the Hatter Department of Marine Technologies, University of Haifa. His research interests include data driven based navigation, novel inertial navigation architectures, autonomous underwater vehicles, sensor fusion, and estimation theory.



navigation architectures, autonomous underwater vehicles, sensor fusion, and estimation theory.